Soliton interaction in the higher-order nonlinear Schrödinger equation investigated with Hirota's bilinear method

Wen-Jun Liu,[1] Bo Tian,[1,2,3,*] Hai-Qiang Zhang,[1] Li-Li Li,[1] and Yu-Shan Xue[1]

[1]*School of Science, P. O. Box 122, Beijing University of Posts and Telecommunications, Beijing 100876, China*

[2]*State Key Laboratory of Software Development Environment, Beijing University of Aeronautics and Astronautics, Beijing 100083, China*

[3]*Key Laboratory of Optical Communication and Lightwave Technologies, Ministry of Education, Beijing University of Posts and Telecommunications, Beijing 100876, China*

(Received 18 January 2008; revised manuscript received 18 April 2008; published 20 June 2008)

The soliton interaction is investigated based on solving the higher-order nonlinear Schrödinger equation with the effects of third-order dispersion, self-steepening, and stimulated Raman scattering. By using Hirota's bilinear method, the analytic one-, two-, and three-soliton solutions of this model are obtained. According to those solutions, the relevant properties and features of physical and optical interest are illustrated. The results of this paper will be valuable to the study of signal amplification and pulse compression.

DOI: 10.1103/PhysRevE.77.066605 PACS number(s): 05.45.Yv, 42.65.Tg, 42.81.Dp, 42.65.Re

I. INTRODUCTION

It has been predicted theoretically in Ref. [1] that an optical pulse in the dielectric fiber can form a solitary wave due to the balance between the nonlinear effect and the group-velocity dispersion (GVD) in the anomalous dispersion regime, and the optical soliton has been reported experimentally in Ref. [2]. Since then, the study of the optical soliton has always been attractive and active, and great progress has been made in both theoretical and experimental research [3–7]. In recent years, to enhance the capacity of high bit rate and long-distance optical communication systems [8], the emphasis is placed on the study of the propagation of ultrashort optical pulses with a subpicosecond (femtosecond) width. In addition, it is of considerable practical importance to investigate higher-order nonlinear effects such as the third-order dispersion (TOD), self-steepening (SS), and stimulated Raman scattering (SRS).

It is well known that the time interval between two neighboring bits or pulses determines the capacity of the optical communication systems, and the stability of two neighboring pulses affects the propagation distance [9]. Namely, the smaller the spacing between the two neighboring pulses, the greater the capacity of the system will be, and the better the stability of pulses, the farther the transmission distance will be. Thereby, if a certain interval between two solitons exists in the system, they will interact mutually. This phenomenon is the interaction between two solitons.

Generally speaking, in the optical soliton communication system, the transmission of information is usually in the form of a large number of soliton pulse series. In this case, these solitons will inevitably interact which directly affects the quality and capacity of the system. Therefore, in the system design, the interaction of solitons is one of the most important issues that need to be considered. According to Ref. [10], when two adjacent solitons have a small interval, there will be interaction between them. Soliton interaction will lead to pulse distortion, transmission characteristic deterioration, transmission rate decrease, and transmission distance shortening. Thereby, the performance of soliton transmission system will be degraded. In order to avoid such kind of soliton mutual interaction, in principle, we can increase the distance between them, but this will restrict the capacity of the system. Actually, the interaction of solitons has been studied widely [11,12] and a series of methods to inhibit such interaction have been reported [13–15]. However, we notice that there has not been much discussion on the interaction of the femtosecond solitons based on the special analytic soliton solutions obtained via Hirota's bilinear method. Therefore, in this paper, we are devoted to investigating the interaction of the femtosecond solitons analytically which is described by the high-order nonlinear Schrödinger (HNLS) equation [16,17]

$$A_z + \frac{\alpha}{2}A + \frac{i}{2}\beta_2 A_{TT} - i\gamma|A|^2A - \frac{\beta_3}{6}A_{TTT} + \frac{\gamma}{\omega_0}(|A|^2A)_T - \gamma T_R A|A|_T^2 = 0, \quad (1)$$

where A is a complex function of z and T, and the subscripts z and T denote the partial derivatives with respect to the distance and time. β_3 is the TOD coefficient, ω_0 is the carrier frequency, α is the attenuation constant, and T_R is the Raman resonant time constant.

Nowadays, with the in-depth study of the interaction of solitons, it has been found that the solitons in the process of interaction can be used in the energy conversion and the pulse compression [18–20]. An attractive feature of the interaction is that solitons during interaction can transform energy, and this has brought increasing interest in studying the process of the interaction which can amplify the solitons without using other techniques. The major virtue of this type of collision-based amplification process is that it does not induce any noise, for it does not require any external amplification medium [19]. However, this research is generally either based on the standard nonlinear Schrödinger (NLS) equation or the standard coupled nonlinear Schrödinger (CNLS) equations.

*Corresponding author. gaoyt@public.bta.net.cn

Being motivated by the above intriguing aspects, in the present work, we carry out a detailed study on the soliton collision dynamics in the HNLS equation. The Hirota's method based on the computerized symbolic computation [21–23] has made it exercisable to solve the HNLS equation under investigation. In particular, via the obtained soliton solutions, we point out that the adjacent solitons can be controlled appropriately in the process of the interaction, provided that the soliton parameters satisfy certain conditions. An important character of the collision process of the solitons is that in the two solitons case, after collision, one of the solitons can gain energy from the other.

The structure of the present paper is as follows. In Sec. II, with the aid of symbolic computation, the bilinear form for the HNLS equation is acquired by use of Hirota's bilinear method. In Sec. III, (a) the one-soliton solution, (b) the two-soliton solution, and (c) the three-soliton solution are explicitly presented based on its bilinear form, and the detailed analysis of the solitons via the obtained soliton solutions are illustrated. Finally, our conclusions are given in Sec. IV.

II. BILINEAR FORM FOR THE HNLS EQUATION

In the anomalous dispersion regime ($\beta_2<0$), considering $\beta_3<0$ and $\alpha L \ll 1$, where L is the fiber length and α is negligible [9], Eq. (1) takes the form in normalized coordinates

$$u_\xi - \frac{i}{2}u_{\tau\tau} - iN^2|u|^2u + \frac{1}{6}L_H u_{\tau\tau\tau} + sN^2(|u|^2u)_\tau - \tau_R N^2 u|u|_\tau^2 = 0, \tag{2}$$

where u is the normalized amplitude and

$$A = \sqrt{P_0}u, \quad L_D = \frac{T_0^2}{|\beta_2|}, \quad L_D' = \frac{T_0^3}{|\beta_3|}, \quad L_{\mathrm{NL}} = \frac{1}{\gamma P_0}, \tag{3}$$

$$\xi = \frac{z}{L_D}, \quad L_H = \frac{L_D}{L_D'}, \quad \tau_R = \frac{T_R}{T_0}, \quad \tau = \frac{T}{T_0} = \frac{t - z/v_g}{T_0},$$

$$N^2 = \frac{L_D}{L_{\mathrm{NL}}} = \frac{\gamma P_0 T_0^2}{|\beta_2|}, \quad s = \frac{1}{\omega_0 T_0},$$

in which P_0 is the peak power of the incident pulse, τ and ξ, respectively, represent the normalized time and the normalized propagation distance, L_D is the dispersion length, L_{NL} the nonlinear length, v_g the group velocity, ω_0 the carrier frequency, N the soliton order, and L_D' a dispersion length associated with the TOD. The parameters s and τ_R account for, respectively, the effects of SS and SRS.

By introducing the dependent variable transformation [24]

$$u = \frac{g(\xi,\tau)}{f(\xi,\tau)}, \tag{4}$$

where $g(\xi,\tau)$ is a complex differentiable function and $f(\xi,\tau)$ is a real one, after some symbolic manipulations, the bilinear form of Eq. (2) is expressed as

$$\left(D_\xi - \frac{i}{2}D_\tau^2 + \frac{1}{6}L_H D_\tau^3\right) g \cdot f = 0, \tag{5}$$

$$D_\tau^2 f \cdot f = 2N^2|g|^2, \tag{6}$$

with the coefficient constraint $L_H = s = \tau_R$. Here, Hirota's bilinear operators D_ξ and D_τ [25,26] are defined by

$$D_\xi^m D_\tau^n (a \cdot b) = \left(\frac{\partial}{\partial\xi} - \frac{\partial}{\partial\xi'}\right)^m \left(\frac{\partial}{\partial\tau} - \frac{\partial}{\partial\tau'}\right)^n \times a(\xi,\tau)b(\xi',\tau')|_{\xi'=\xi,\tau'=\tau}. \tag{7}$$

Equations (5) and (6) can be solved by introducing the following power series expansions for g and f:

$$g = \epsilon g_1 + \epsilon^3 g_3 + \epsilon^5 g_5 + \cdots, \tag{8}$$

$$f = 1 + \epsilon^2 f_2 + \epsilon^4 f_4 + \epsilon^6 f_6 + \cdots, \tag{9}$$

where ϵ is a formal expansion parameter. Substituting Eqs. (8) and (9) into Eqs. (5) and (6) and equating coefficients of the same powers of ϵ to zero can yield the recursion relations for $f_n(\xi,\tau)$ and $g_n(\xi,\tau)$ $(n=1,2,\ldots)$.

III. SOLITON SOLUTIONS FOR THE HNLS EQUATION

In the above section, we have obtained the bilinear form for the HNLS equation. In order to analytically study the process of the interaction of solitons, next we will give the one-, two-, and three-soliton solutions from the bilinear Eqs. (5) and (6) and present the related graphics of them to explain the physical relevance of soliton solutions. We assume that the input pulse is a fundamental soliton pulse of the form

$$A(0,\tau) = N\,\mathrm{sech}(\tau), \tag{10}$$

which has a wavelength of 1.55 μm and an initial T_{FWHM} ($T_{\mathrm{FWHM}} = 1.763T_0$) of 150 fs.

A. One-soliton solution

To obtain the one-soliton solution for Eq. (2), we assume that

$$g_1 = e^\theta, \tag{11}$$

where $\theta = \psi(\xi) + \eta\tau + \varphi_0$ with η as an arbitrary complex parameter, φ_0 as a real constant, and $\psi(\xi)$ as a differentiable function to be determined. Substituting $g(\xi,\tau)$ into the resulting set of linear partial differential equations, and after some calculations, $\psi(\xi)$ is determined to be

$$\psi(\xi) = \left(\frac{i}{2}\eta^2 - \frac{L_H}{6}\eta^3\right)\xi$$

and

$$f_2 = \frac{N^2 e^{\theta+\theta^*}}{(\eta+\eta^*)^2}, \quad g_n(\xi,\tau) = 0 \quad (n=3,5,\ldots), \tag{12}$$

$$f_n(\xi,\tau) = 0 \quad (n=4,6,\ldots).$$

Without loss of generality, we set $\epsilon = 1$. Thus, the one-soliton solution can be explicitly expressed as

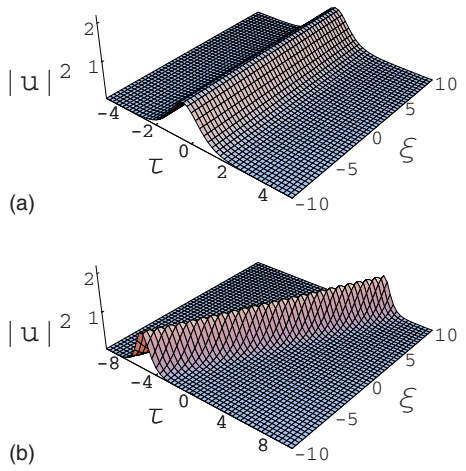

FIG. 1. (Color online) Intensity profiles of the soliton solution expressed via solution (13). The parameters adopted here are $\varphi_0=1$, $N=1$, $L_H=0.01$ with (a) $\eta=1$, (b) $\eta=1+i$.

$$u=\frac{g}{f}=\frac{g_1}{1+f_2}=\frac{e^{\theta}}{1+\frac{N^2e^{\theta+\theta^*}}{(\eta+\eta^*)^2}}, \tag{13}$$

where the asterisk denotes the complex conjugate.

According to Eq. (13), we will get the graphics shown in Fig. 1. Figure 1 illustrates the pulse propagation of the fundamental soliton along the distance ξ with suitable choice of the parameters in Eq. (13). The phase of the soliton will be changed if we choose the different values of η. In this case, $\eta=1$ in Fig. 1(a) and $\eta=1+i$ in Fig. 1(b), respectively. However, they both transmit stably without distortion of the soliton shape. At that time, the effect of self-phase modulation (SPM) can cancel the effect of anomalous GVD perfectly. These results indicate that only η influences the phase of the fundamental soliton but the soliton properties will not be affected if we just change the value of η.

B. Two-soliton solution

The fundamental soliton cannot interact with other solitons in a single communication system in the ideal conditions as discussed in section A. Whereas, there are always multiple signals in the high bit rate and long-distance optical communication system. Therefore, it is necessary to study the multisoliton transmission in the system. In this section, we mainly pay our attention to the interaction between two solitons. At first, to derive the two-soliton solution, we take

$$g=g_1+g_3, \quad f=1+f_2+f_4, \tag{14}$$

where $g_1=e^{\theta_1}+e^{\theta_2}$, $\theta_j=\psi_j(\xi)+\eta_j\tau+\varphi_j(j=1,2)$ with η_j as arbitrary complex parameters, φ_j as real constants and

$$\psi_j(\xi)=\left(\frac{i}{2}\eta_j^2-\frac{L_H}{6}\eta_j^3\right)\xi. \tag{15}$$

Then, by solving the resulting linear partial differential equations recursively, we can write the explicit form of the two-soliton solution as

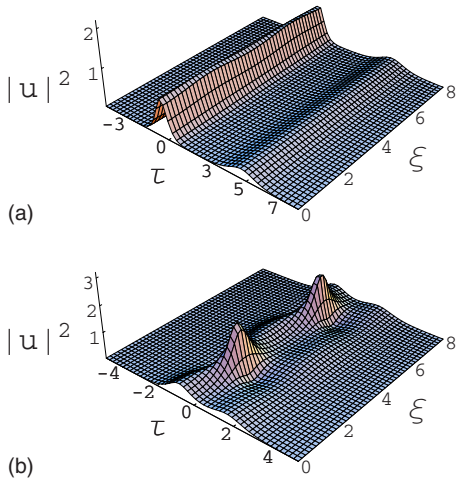

FIG. 2. (Color online) Intensity profiles of the two-soliton solution expressed via solution (16). The parameters adopted here are $\eta_1=2$, $\eta_2=1$, $\varphi_1=1.5$, $N=2$, $L_H=0.01$ with (a) $\varphi_2=-2.5$, (b) $\varphi_2=0.5$.

$$u=\frac{g}{f}=\frac{g_1+g_3}{1+f_2+f_4}=\frac{e^{\theta_1}+e^{\theta_2}+A_{21}e^{\theta_1+\theta_2+\theta_1^*}+A_{22}e^{\theta_1+\theta_2+\theta_2^*}}{D_1}, \tag{16}$$

where

$$D_1=1+B_{21}e^{\theta_1+\theta_1^*}+B_{22}e^{\theta_2+\theta_1^*}+B_{23}e^{\theta_1+\theta_2^*}+B_{24}e^{\theta_2+\theta_2^*}+C_{21}e^{\theta_1+\theta_2+\theta_1^*+\theta_2^*}, \tag{17}$$

with

$$A_{2j}=\sum_{l=1}^{2}\frac{N^2(\eta_l-\eta_j)^2}{(\eta_j+\eta_j^*)^2(\eta_l+\eta_j^*)^2} \quad (l\neq j, \quad j=1,2),$$

$$B_{21}=\frac{N^2}{(\eta_1+\eta_1^*)^2}, \quad B_{22}=\frac{N^2}{(\eta_2+\eta_1^*)^2},$$

$$B_{23}=\frac{N^2}{(\eta_1+\eta_2^*)^2}, \quad B_{24}=\frac{N^2}{(\eta_2+\eta_2^*)^2},$$

$$C_{21}=\frac{N^4(\eta_1-\eta_2)^2(\eta_1^*-\eta_2^*)^2}{(\eta_1+\eta_1^*)^2(\eta_2+\eta_2^*)^2(\eta_1+\eta_2^*)^2(\eta_2+\eta_1^*)^2}.$$

With the suitable choice of the parameters in Eq. (16), we get Fig. 2. We choose the same value of η_1 and η_2 but different φ_2 in Figs. 2(a) and 2(b). In this case, the phases of the two solitons are the same and two sets of parallel solitons are obtained. In Fig. 2(a), the two-soliton pulses do not interact with each other and propagate stably along the optical fiber with a constant separation between them even if the propagation distance grows long enough. However, if we reduce the interval between the two solitons which is primarily reflected in the revised value of φ_2, as shown in Fig. 2(b), interaction occurs. The pulses follow a periodic evolution pattern in the anomalous dispersion regime as they propagate along the fiber. Namely, by selecting suitable ini-

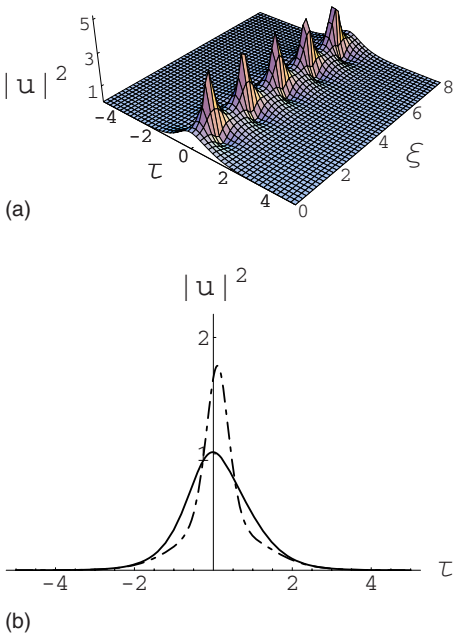

FIG. 3. (Color online) (a) Intensity profiles of the two-soliton solution expressed via solution (16) with $\eta_1=3$, $\eta_2=1$, $\varphi_1=1.5$, $\varphi_2=0.5$, $N=2$, $L_H=0.01$. (b) Comparison between the input pulse and the second-order soliton at $\xi=2$.

tial separation between two solitons, they can propagate separately without interaction. For the case of Fig. 2(b), by choosing the proper values of η_1 and η_2, e.g., $\eta_1=3$ and $\eta_2=1$, the compressed soliton pulse will be acquired, as shown in Fig. 3.

Figure 3 demonstrates that the two solitons evolve into the second-order soliton and soliton-effect pulse compression phenomenon occurs in this case. From Fig. 3(a), we can see that the two-order soliton contracts to a fraction of its initial width at first, and then merges again to recover the original shape. These changes mainly result from the mutual interaction between the SPM and GVD. In order to show the compressed soliton pulse better, we generate its transverse graphics Fig. 3(b). The solid curve in Fig. 3(b) represents the initial shape of the input pulse which is symmetric at $\xi=0$ and the dashed curve represents the pulse at $\xi=2$.

In the cases discussed above, η_1 and η_2 are both real constants and the input pulses are parallel to each other, while in following Fig. 4, the values of η_1 and η_2 will be considered as complex. The two input pulses do not keep the same phase and have an angle. The size of the angle between two pulses is determined by η_1 and η_2. Now, it is of great value to investigate the collision process of these two solitons. In Fig. 4(a) with $\eta_1=1+i$ and $\eta_2=1.1-i$, a head-on collision of the two solitons is illustrated. At the moment of collision they exchange their energy along with a phase shift. The left-hand soliton gets enhanced in its amplitude while the other one is suppressed. The two solitons collide unperiodically after being input into the optical fiber for distances, and are well separated before and after collision. And this is particularly evident after collision: the two solitons separate with larger and larger interval along the propagation direction. In addition, the pulse width of both of the two solitons

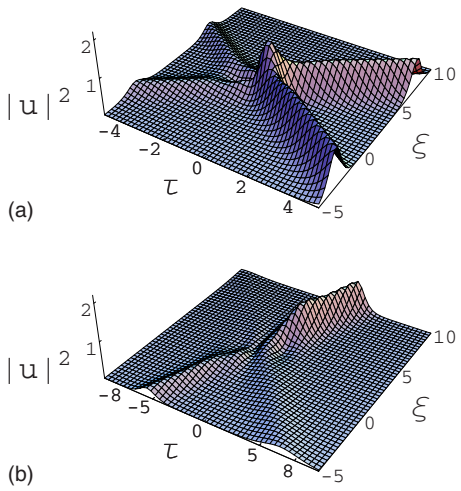

FIG. 4. (Color online) Intensity profiles of the two-soliton solution expressed via solution (16). The parameters adopted here are: $\varphi_1=3$, $\varphi_2=-1$, $N=2$, $L_H=0.01$ with (a) $\eta_1=1+i$, $\eta_2=1.1-i$, (b) $\eta_1=1+0.5i$, $\eta_2=0.5-i$.

decreases while their amplitude increases at the beginning of collision, then they exchange their energy and the pulse expands with decreasing energy after propagating in the fiber for distances. Compared with Fig. 4(a), Fig. 4(b) illustrates another energy exchange phenomenon, in which the amplitude of one interacting soliton nearly becomes zero after the collision.

From Eq. (2), the energy conservation law can be obtained as

$$(|u|^2)_\xi + \left[\frac{i}{2}(u_\tau^* u - u_\tau u^*) + \frac{1}{6}L_H(|u|_{\tau\tau}^2 - 3u_\tau^* u_\tau) + \left(\frac{3}{2}sN^2 - \tau_R N^2\right)|u|^4\right]_\tau = 0. \tag{18}$$

In Fig. 4, both of the two solitons comply with the energy conservation law before and after collision, which means that the collision scenario shown in Fig. 4 may be viewed as an amplification process in which one of the solitons represents a signal (or data carrier) while the other soliton represents an energy reservoir (pump). The main virtue of this amplification process is that it does not require any external amplification medium, and therefore the amplification of the soliton does not induce any noise.

C. Three-soliton solution

According to the above procedure of obtaining the one- and two-soliton solutions, we can proceed to construct the three-soliton solution for Eq. (2) as below:

$$u = \frac{g}{f} = \frac{g_1 + g_3 + g_5}{1 + f_2 + f_4 + f_6}, \tag{19}$$

where

$$g_1 = e^{\theta_1} + e^{\theta_2} + e^{\theta_3}, \quad g_3 = A_{31}e^{\theta_1+\theta_2+\theta_1^*} + A_{32}e^{\theta_1+\theta_3+\theta_1^*} + A_{33}e^{\theta_1+\theta_2+\theta_2^*} + A_{34}e^{\theta_2+\theta_3+\theta_2^*} + A_{35}e^{\theta_1+\theta_3+\theta_3^*} + A_{36}e^{\theta_2+\theta_3+\theta_3^*} + A_{37}e^{\theta_2+\theta_3+\theta_1^*} + A_{38}e^{\theta_1+\theta_3+\theta_2^*} + A_{39}e^{\theta_1+\theta_2+\theta_3^*}, \tag{20}$$

$$g_5 = M_{31}e^{\theta_1+\theta_2+\theta_3+\theta_1^*+\theta_2^*} + M_{32}e^{\theta_1+\theta_2+\theta_3+\theta_2^*+\theta_3^*} + M_{33}e^{\theta_1+\theta_2+\theta_3+\theta_1^*+\theta_3^*},$$

$$f_2 = B_{31}e^{\theta_1+\theta_1^*} + B_{32}e^{\theta_2+\theta_2^*} + B_{33}e^{\theta_3+\theta_3^*} + B_{34}e^{\theta_1+\theta_2^*} + B_{35}e^{\theta_2+\theta_1^*} + B_{36}e^{\theta_1+\theta_3^*} + B_{37}e^{\theta_3+\theta_1^*} + B_{38}e^{\theta_2+\theta_3^*} + B_{39}e^{\theta_3+\theta_2^*},$$

$$f_4 = C_{31}e^{\theta_1+\theta_2+\theta_1^*+\theta_2^*} + C_{32}e^{\theta_1+\theta_3+\theta_1^*+\theta_3^*} + C_{33}e^{\theta_2+\theta_3+\theta_2^*+\theta_3^*} + C_{34}e^{\theta_1+\theta_2+\theta_1^*+\theta_3^*} + C_{35}e^{\theta_1+\theta_3+\theta_1^*+\theta_2^*} + C_{36}e^{\theta_1+\theta_2+\theta_2^*+\theta_3^*} + C_{37}e^{\theta_2+\theta_3+\theta_1^*+\theta_2^*} + C_{38}e^{\theta_1+\theta_3+\theta_2^*+\theta_3^*} + C_{39}e^{\theta_2+\theta_3+\theta_1^*+\theta_3^*},$$

$$f_6 = Q_3e^{\theta_1+\theta_2+\theta_3+\theta_1^*+\theta_2^*+\theta_3^*},$$

$$A_{31} = N^2(\eta_1-\eta_2)^2(\eta_1+\eta_1^*)^2(\eta_2+\eta_1^*)^2, \quad A_{32} = \frac{N^2(\eta_1-\eta_3)^2}{(\eta_1+\eta_1^*)^2(\eta_3+\eta_1^*)^2}, \quad A_{33} = \frac{N^2(\eta_1-\eta_2)^2}{(\eta_1+\eta_2^*)^2(\eta_2+\eta_2^*)^2},$$

$$A_{34} = \frac{N^2(\eta_2-\eta_3)^2}{(\eta_2+\eta_2^*)^2(\eta_3+\eta_2^*)^2}, \quad A_{35} = \frac{N^2(\eta_1-\eta_3)^2}{(\eta_1+\eta_3^*)^2(\eta_3+\eta_3^*)^2}, \quad A_{36} = \frac{N^2(\eta_2-\eta_3)^2}{(\eta_2+\eta_3^*)^2(\eta_3+\eta_3^*)^2},$$

$$A_{37} = \frac{N^2(\eta_2-\eta_3)^2}{(\eta_2+\eta_1^*)^2(\eta_3+\eta_1^*)^2}, \quad A_{38} = \frac{N^2(\eta_1-\eta_3)^2}{(\eta_1+\eta_2^*)^2(\eta_3+\eta_2^*)^2}, \quad A_{39} = \frac{N^2(\eta_1-\eta_2)^2}{(\eta_1+\eta_3^*)^2(\eta_2+\eta_3^*)^2},$$

$$B_{31} = \frac{N^2}{(\eta_1+\eta_1^*)^2}, \quad B_{32} = \frac{N^2}{(\eta_2+\eta_2^*)^2}, \quad B_{33} = \frac{N^2}{(\eta_3+\eta_3^*)^2}, \quad B_{34} = \frac{N^2}{(\eta_1+\eta_2^*)^2}, \quad B_{35} = \frac{N^2}{(\eta_2+\eta_1^*)^2}, \quad B_{36} = \frac{N^2}{(\eta_1+\eta_3^*)^2},$$

$$B_{37} = \frac{N^2}{(\eta_3+\eta_1^*)^2}, \quad B_{38} = \frac{N^2}{(\eta_2+\eta_3^*)^2}, \quad B_{39} = \frac{N^2}{(\eta_3+\eta_2^*)^2}, \quad C_{31} = \frac{N^4(\eta_1-\eta_2)^2(\eta_1^*-\eta_2^*)^2}{(\eta_1+\eta_1^*)^2(\eta_1+\eta_2^*)^2(\eta_2+\eta_1^*)^2(\eta_2+\eta_2^*)^2},$$

$$C_{32} = \frac{N^4(\eta_1-\eta_3)^2(\eta_1^*-\eta_3^*)^2}{(\eta_1+\eta_1^*)^2(\eta_1+\eta_3^*)^2(\eta_3+\eta_1^*)^2(\eta_3+\eta_3^*)^2}, \quad C_{33} = \frac{N^4(\eta_2-\eta_3)^2(\eta_2^*-\eta_3^*)^2}{(\eta_2+\eta_2^*)^2(\eta_2+\eta_3^*)^2(\eta_3+\eta_2^*)^2(\eta_3+\eta_3^*)^2},$$

$$C_{34} = \frac{N^4(\eta_1-\eta_2)^2(\eta_1^*-\eta_3^*)^2}{(\eta_1+\eta_1^*)^2(\eta_1+\eta_3^*)^2(\eta_2+\eta_1^*)^2(\eta_2+\eta_3^*)^2}, \quad C_{35} = \frac{N^4(\eta_1-\eta_3)^2(\eta_1^*-\eta_2^*)^2}{(\eta_1+\eta_1^*)^2(\eta_1+\eta_2^*)^2(\eta_3+\eta_1^*)^2(\eta_3+\eta_2^*)^2},$$

$$C_{36} = \frac{N^4(\eta_1-\eta_2)^2(\eta_2^*-\eta_3^*)^2}{(\eta_1+\eta_2^*)^2(\eta_1+\eta_3^*)^2(\eta_2+\eta_2^*)^2(\eta_2+\eta_3^*)^2}, \quad C_{37} = \frac{N^4(\eta_2-\eta_3)^2(\eta_1^*-\eta_2^*)^2}{(\eta_2+\eta_1^*)^2(\eta_2+\eta_2^*)^2(\eta_3+\eta_1^*)^2(\eta_3+\eta_2^*)^2},$$

$$C_{38} = \frac{N^4(\eta_1-\eta_3)^2(\eta_2^*-\eta_3^*)^2}{(\eta_1+\eta_2^*)^2(\eta_1+\eta_3^*)^2(\eta_3+\eta_2^*)^2(\eta_3+\eta_3^*)^2}, \quad C_{39} = \frac{N^4(\eta_2-\eta_3)^2(\eta_1^*-\eta_3^*)^2}{(\eta_2+\eta_1^*)^2(\eta_2+\eta_3^*)^2(\eta_3+\eta_1^*)^2(\eta_3+\eta_3^*)^2},$$

$$M_{31} = \frac{N^4(\eta_1-\eta_2)^2(\eta_1-\eta_3)^2(\eta_2-\eta_3)^2(\eta_1^*-\eta_2^*)^2}{(\eta_1+\eta_1^*)^2(\eta_1+\eta_2^*)^2(\eta_2+\eta_1^*)^2(\eta_2+\eta_2^*)^2(\eta_3+\eta_1^*)^2(\eta_3+\eta_2^*)^2},$$

$$M_{32} = \frac{N^4(\eta_1-\eta_2)^2(\eta_1-\eta_3)^2(\eta_2-\eta_3)^2(\eta_2^*-\eta_3^*)^2}{(\eta_1+\eta_2^*)^2(\eta_1+\eta_3^*)^2(\eta_2+\eta_2^*)^2(\eta_2+\eta_3^*)^2(\eta_3+\eta_2^*)^2(\eta_3+\eta_3^*)^2},$$

$$M_{33} = \frac{N^4(\eta_1-\eta_2)^2(\eta_1-\eta_3)^2(\eta_2-\eta_3)^2(\eta_1^*-\eta_3^*)^2}{(\eta_1+\eta_1^*)^2(\eta_1+\eta_3^*)^2(\eta_2+\eta_1^*)^2(\eta_2+\eta_3^*)^2(\eta_3+\eta_1^*)^2(\eta_3+\eta_3^*)^2},$$

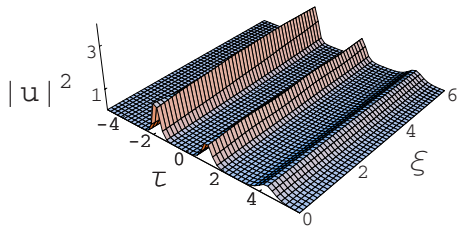

FIG. 5. (Color online) Intensity profiles of the three-soliton solution expressed via solution (19). The parameters adopted here are $\eta_1=2$, $\eta_2=3$, $\eta_3=4$, $\varphi_1=-3$, $\varphi_2=1$, $\varphi_3=8$, $N=3$, $L_H=0.01$.

$$Q_3 = \frac{N^6(\eta_1-\eta_2)^2(\eta_1-\eta_3)^2(\eta_2-\eta_3)^2}{(\eta_1+\eta_1^*)^2(\eta_1+\eta_2^*)^2(\eta_1+\eta_3^*)^2(\eta_2+\eta_1^*)^2(\eta_2+\eta_2^*)^2} \times \frac{(\eta_1^*-\eta_2^*)^2(\eta_1^*-\eta_3^*)^2(\eta_2^*-\eta_3^*)^2}{(\eta_2+\eta_3^*)^2(\eta_3+\eta_1^*)^2(\eta_3+\eta_2^*)^2(\eta_3+\eta_3^*)^2}, \quad (21)$$

with $\theta_j=\psi_j(\xi)+\eta_j\tau+\varphi_j(j=1,2,3)$, η_j as arbitrary complex parameters, φ_j as real constants and

$$\psi_j(\xi) = \left(\frac{i}{2}\eta_j^2 - \frac{L_H}{6}\eta_j^3\right)\xi.$$

When $N=3$, according to Eq. (19), by suitable choices of the parameters of φ_1, φ_2, and φ_3, we have the intensity profiles of the three-soliton solution expressed via Eq. (19), as shown in Fig. 5.

Similar to the two soliton pulses, the parallel three soliton pulses transmit stably without interaction with each other and propagate along the optical fiber with a constant separation among them. However, when we revise the values of φ_1, φ_2, and φ_3, the interactions of the solitons corresponding to the revision is shown in Fig. 6.

The interaction scenario shown in Fig. 6(a) can be explained by the relative distance among three solitons. The

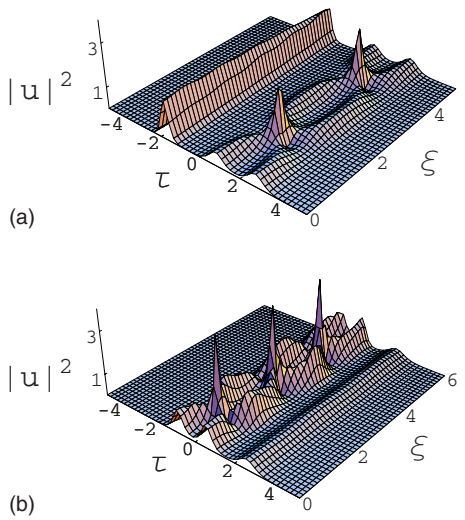

FIG. 6. (Color online) Intensity profiles of the three-soliton solution expressed via solution (19). The parameters adopted here are $\eta_1=2$, $\eta_2=3$, $\eta_3=4$, $N=3$, $L_H=0.01$ with (a) $\varphi_1=0.5$, $\varphi_2=1$, $\varphi_3=8$, (b) $\varphi_1=0.6$, $\varphi_2=2.8$, $\varphi_3=3.15$.

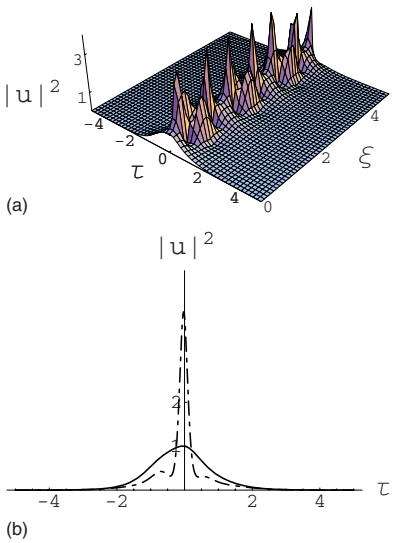

FIG. 7. (Color online) (a) Intensity profiles of the three-soliton solution expressed via solution (19) with $\eta_1=1$, $\eta_2=3$, $\eta_3=5$, $\varphi_1=0.6$, $\varphi_2=2.8$, $\varphi_3=3.15$, $N=3$, $L_H=0.01$; (b) comparison between the input pulse and the third-order soliton at $\xi=2$.

relative distance between the right hand soliton and the middle one is smaller than that between the left hand one and the middle one, thus, the right hand soliton and the middle one interact strongly while the left hand soliton can propagate undistorted. The reason why the physical phenomenon occurring in Fig. 6(b) can also be illustrated by the above explanation on relative distance among them. Compared with Fig. 6(b), if keeping the values of φ_1, φ_2, and φ_3 and changing the values of η_1, η_2, and η_3 properly, we can draw the graphics shown in Fig. 7.

As shown in Fig. 7, these three solitons evolve into a third-order soliton. Soliton-effect pulse compression phenomenon also occurs in this case. Figure 7(a) displays the periodic evolution of the third-order soliton. As the pulse propagates along the fiber, it splits into two distinct pulses, contracts to a fraction of its initial width, and then merges again to recover the original shape. Compared with the second-order soliton in Fig. 3(b), the level of compression is obviously enhanced which can be seen from Fig. 7(b). The reason for the varying shape and the enhanced level of compression can be traced to the soliton order N. It is clear that higher order of the soliton will enhance the amplitude of the soliton and vice versa. However, the increase of the soliton order N will result in the reduction of the quality of the pulses originally compressed. Fortunately, there exists a simple and feasible technique which can significantly improve the pulse quality achieved by the soliton-effect pulse compression technique.

IV. CONCLUSIONS

In this paper, we have obtained the analytic soliton solutions for the HNLS equation, i.e., Eq. (2), by directly applying Hirota's bilinear method. We have analyzed the propagation of the one, two, and three solitons in detail. According to expression (13), the fundamental soliton pulse could transmit

stably without distortion of the soliton shape in a certain range with suitable choices of the parameters. Depending upon different choices of the soliton parameters, the multisoliton solutions have different applications. If η is a real constant, the two and three solitons can be used for pulse compression in ultra-high-rate and long-distance optical communication systems. Moreover, with the increase of the order of the soliton, the compression will become intense. While η is chosen as complex, we can infer from the collision process that the relative phase difference of those solitons changes in contrast with the one of the input solitons. The centers of solitons move away from the original positions, at the same time, the solitons undergo fascinating energy exchange in the two soliton system. By virtue of this energy exchange property, it is feasible to promote the collision process to the rank of a highly efficient amplification process without noise generation. The results of this paper will be of certain value to the study on signal amplification and pulse compression.

ACKNOWLEDGMENTS

We express our sincere thanks to Professor Y. T. Gao and other members of our discussion group for their valuable comments. This work has been supported by the National Natural Science Foundation of China under Grant No. 60772023 and No. 60372095, by the Key Project of the Chinese Ministry of Education (Grant No. 106033), by the Open Fund of the State Key Laboratory of Software Development Environment under Grant No. SKLSDE-07-001, Beijing University of Aeronautics and Astronautics, by the National Basic Research Program of China (973 Program) under Grant No. 2005CB321901, and by the Specialized Research Fund for the Doctoral Program of Higher Education (Grant No. 20060006024), Chinese Ministry of Education.

[1] A. Hasegawa and F. Tappert, Appl. Phys. Lett. **23**, 142 (1973); A. Hasegawa and F. Tappert, *ibid.* **23**, 171 (1973).
[2] L. F. Mollenauer, R. H. Stolen, and J. P. Gordon, Phys. Rev. Lett. **45**, 1095 (1980).
[3] B. Tian, W. R. Shan, C. Y. Zhang, G. M. Wei, and Y. T. Gao, Eur. Phys. J. B **47**, 329 (2005); B. Tian and Y. T. Gao, Phys. Lett. A **342**, 228 (2005); B. Tian and Y. T. Gao, *ibid.* **359**, 241 (2006); B. Tian, Y. T. Gao, and H. W. Zhu, *ibid.* **366**, 223 (2007).
[4] J. Li, H. Q. Zhang, T. Xu, Y. X. Zhang, and B. Tian, J. Phys. A **40**, 13299 (2007); A. Mahalingam and T. Alagesan, Chaos, Solitons Fractals **25**, 319 (2005).
[5] G. L. Lamb, Jr., *Elements of Soliton Theory* (Wiley, New York, 1980).
[6] H. Toda, Y. Furukawa, T. Kinoshita, Y. Kodama, and A. Hasegawa, IEEE Photon. Technol. Lett. **9**, 1415 (1997); T. Kanna, E. N. Tsoy, and N. Akhmediev, Phys. Lett. A **330**, 224 (2004); F. K. Abdullaev and J. Garnier, Phys. Rev. E **72**, 035603(R) (2005).
[7] T. Xu, C. Y. Zhang, G. M. Wei, J. Li, X. H. Meng, and B. Tian, Eur. Phys. J. B **55**, 323 (2007); H. Q. Zhang, X. H. Meng, T. Xu, L. L. Li, and B. Tian, Phys. Scr. **75**, 537 (2007).
[8] K. C. Chan and H. F. Liu, IEEE J. Quantum Electron. **31**, 2226 (1995).
[9] G. P. Agrawal, *Nonlinear Fiber Optics*, 3rd ed. (Academic, San Diego, CA, 2002).
[10] J. P. Gordon, Opt. Lett. **8**, 596 (1983).
[11] C. Desem and P. L. Chu, Electron. Lett. **23**, 260 (1987).
[12] V. V. Afanasjev, V. A. Vysloukh, and V. N. Serkin, Opt. Lett. **15**, 489 (1990).
[13] P. L. Chu and C. Desem, Electron. Lett. **19**, 956 (1983).
[14] D. Anderson and M. Lisak, Opt. Lett. **11**, 174 (1986).
[15] P. L. Chu and C. Desem, Electron. Lett. **21**, 1133 (1985).
[16] Y. Kodama, J. Stat. Phys. **39**, 597 (1985).
[17] Y. Kodama and A. Hasegawa, IEEE J. Quantum Electron. **23**, 510 (1987).
[18] T. Kanna and M. Lakshmanan, Phys. Rev. E **67**, 046617 (2003).
[19] T. Kanna, M. Lakshmanan, P. T. Dinda, and N. Akhmediev, Phys. Rev. E **73**, 026604 (2006).
[20] T. Kanna, M. Vijayajayanthi, and M. Lakshmanan, Phys. Rev. A **76**, 013808 (2007).
[21] M. P. Barnett, J. F. Capitani, J. Von Zur Gathen, and J. Gerhard, Int. J. Quantum Chem. **100**, 80 (2004); Y. T. Gao and B. Tian, Phys. Plasmas **13**, 112901 (2006); Y. T. Gao and B. Tian, Europhys. Lett. **77**, 15001 (2007); Y. T. Gao and B. Tian, Phys. Lett. A **349**, 314 (2006); Y. T. Gao and B. Tian, *ibid.* **361**, 523 (2007); Y. T. Gao and B. Tian, Phys. Plasmas **13**, 120703 (2006).
[22] G. C. Das and J. Sarma, Phys. Plasmas **6**, 4394 (1999); W. P. Hong, Phys. Lett. A **361**, 520 (2007); B. Tian and Y. T. Gao, Eur. Phys. J. D **33**, 59 (2005); B. Tian and Y. T. Gao, Phys. Plasmas **12**, 070703 (2005); B. Tian and Y. T. Gao, *ibid.* **12**, 054701 (2005); B. Tian and Y. T. Gao, Phys. Lett. A **340**, 243 (2005); B. Tian and Y. T. Gao, *ibid.* **340**, 449 (2005); B. Tian and Y. T. Gao, *ibid.* **362**, 283 (2007).
[23] Z. Y. Yan and H. Q. Zhang, J. Phys. A **34**, 1785 (2001); Y. T. Gao, B. Tian, and C. Y. Zhang, Acta Mech. **182**, 17 (2006); B. Tian, G. M. Wei, C. Y. Zhang, W. R. Shan, and Y. T. Gao, Phys. Lett. A **356**, 8 (2006).
[24] R. Hirota, J. Math. Phys. **14**, 805 (1973).
[25] R. Hirota, Phys. Rev. Lett. **27**, 1192 (1971).
[26] J. J. C. Nimmo and N. C. Freeman, J. Phys. A **17**, 1415 (1984).